Supplement of Geosci. Model Dev., 16, 3629–3650, 2023
https://doi.org/10.5194/gmd-16-3629-2023-supplement

Geoscientific Model Development
Open Access

Supplement of

Improving Antarctic Bottom Water precursors in NEMO for climate applications

Katherine Hutchinson et al.

Correspondence to: Katherine Hutchinson (kath.hutchinson@gmail.com)

Supplementary Material

S1 A note on the NEMO namelists

In the Zenodo data repository associated with this manuscript (10.5281/zenodo.7561767), the NEMO reference namelist (namelist_ref), "Open" configuration namelist (namelist_core_ia_cfg) and sea ice namelists (namelist_ice_ref and namelist_ice_cfg) are given. The reference namelist is the default provided with the NEMO code. Unless stated otherwise in the "cfg", the simulation uses the choices selected in the "ref" namelist. The namelist_core_ia_cfg is specific to a global ocean configuration (with modifications adapted to eORCA1) forced by interannual core winds. For more information on all the parameters included in these namelists, please refer to the NEMO reference manual available on Zenodo (10.5281/zenodo.6334656). Of specific interest may be Chapter 6.10 on "Interaction with ice shelves (ISF)" where the various options to represent ice-shelf/ ocean fluxes, heat and salt exchange coefficients and melt parameterization choices are explained.

The differences in namelist_core_ia_cfg for the "Open" and "Closed" cavity runs are listed in Table S1. Note that these differences are minor as the adaptations are made mostly to the input files (explained under "DOMAIN FILES AND INITIAL CONDITIONS" in Zenodo data repository description 10.5281/zenodo.7561767).

Namelist parameter	Brief description	Closed	Open
ln_isfcav_mlt	ice shelf melting into the cavity	false	true
sn_isfpar_fwf	namelist block for freshwater flux from ice shelf melt	Read in fixed freshwater flux from melt as estimated from Depoorter et al. (2013) for all ice shelves	Use a new input file where this freshwater flux is removed in front of FRIS, LCIS and ROSS.
ln_hpg_sco	s-coordinate formulation of pressure gradient	true	false
ln_hpg_isf	s-coordinate formulation of pressure gradient adapted for under ice shelves.	false	true

Table S1 Namelist differences when FRIS, LCIS and ROSS cavities are open.

S2 An alternative methodology to parameterize the effect of tides under the ice shelves

S2.1 Rationale

The influence of tides on ice shelf basal melt is parameterized in NEMO using a constant background kinetic energy, set to the value of 2.5 x 10^{-3} m^2 s^{-2} everywhere (namelist parameter rn_ke0). As discussed in Jourdain et al. (2019), within ice shelf cavities tides play an important role in modulating basal melt by imposing an added current velocity along the ice shelf base. The magnitude of the tidal currents are, however, not constant everywhere, and so a single kinetic energy value (as is the default option in NEMO) can be improved upon by using a two dimensional field. To inform this, we follow the methodology of Jourdain et al. (2019) and use the Circum-Antarctic Tidal Simulation CATS2008 tidal map interpolated onto the eORCA1 grid (Howard et al., 2019). Additionally, some of the NEMO code had to be adapted to allow for this type of tidal parameterization and so the following files were amended: isf_oce.F90, isfcavgam.F90, isfstp.F90, zdfdrg.F90. The simulation was run for 124 years and the differences in melt rate between this simulation and the reference “Open” cavity simulation are presented in Fig. S1.

S2.2 Impact of alternative tidal parameterization on basal melt

Using the two-dimensional CATS tidal atlas to parameterize the effect of tides slightly increases melt for FRIS (total mean melt flux over 1995-2009 of 120 ± 22 Gt/yr) and LCIS (39 ± 8 Gt/yr) and reduces net melt for ROSS (102 ± 18 Gt/yr) compared to results shown in Table 1. In general, the tidal velocities for CATS under FRIS and LCIS are faster than the default constant and for RIS are slower. The spatial differences in yearly basal melt rate can be seen in Fig. S1. The marked differences for FRIS are an increase in melt at the ice shelf front and a decrease within the deep fjords along the grounding line. An explanation for this is that the elevated tidal velocities increase the rate of melting as warm offshore water enters the cavity, causing elevated melt along the western ice shelf front. This water then loses its heat, and thus potential for melt, and slows down as it travels into the southernmost extremities of the cavity where it induces less melt than in the default simulation. The converse is true for RIS where the CATS tidal map shows slower induced velocities than the default parameterization, meaning a decrease in the melt rate all along the ice shelf front. To explore the impact of these changes in melt rate on water mass properties, we also compared with two cross sections across the ice shelf fronts (FRIS February 1995 and RIS February 2000) and found temperature differences of less than 0.1°C and salinity differences of less than 0.05 psu using this alternative method to represent the tidal effect. These plots are not included here as it is impossible to see the difference compared to Figs. 6 and 7 with the naked eye, and another anomaly plot adds no value to the reader.

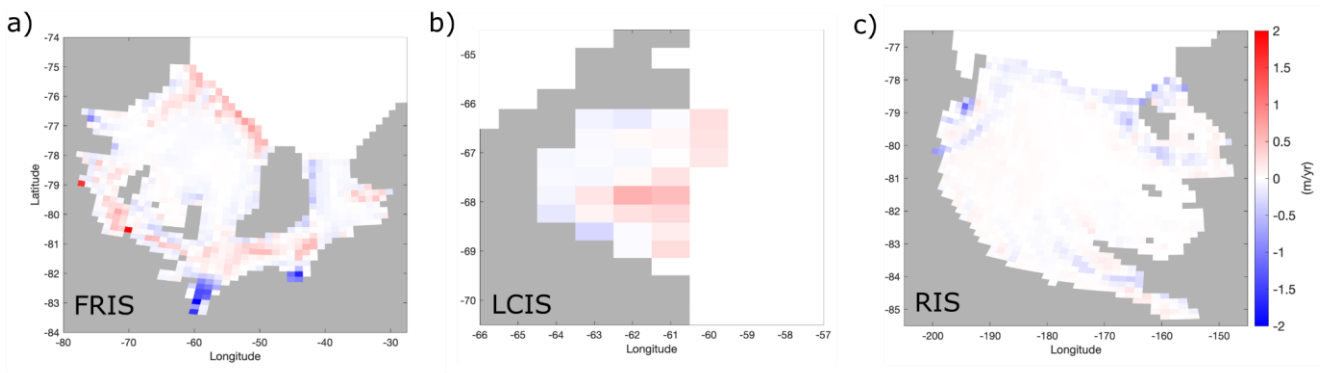

Figure S1. Difference in melt rates (CATS tides - default parameterization) for (a) Filchner-Ronne Ice Shelf, (b) Larsen C Ice Shelf and (c) Ross Ice Shelf. The results are mean values for the model equivalent period 1995-2009. A positive difference indicates more melting for the “CATS tides” run in areas of melt in Figure 4, and less freezing in areas of re-freezing in Figure 4.

S2.3 Conclusion

This simulation using a two dimensional map of tidal velocities informed by CATS2008 shows minor changes in net melt flux for each cavity (<10 Gt/yr) and small adjustments in the melt rate pattern (<2 m/yr). These changes are not as large as one would expect when tides are explicitly simulated as in that case, the basin wide circulation and water mass distribution would be affected. Explicit tides were not explored in this study as the eORCA1 configuration we use is designed for climate applications (explicit tides do not fit this purpose as they contribute too much numerical mixing).

S3 An evaluation of sea ice production and polynya activity in the NEMO simulations

In this section, we analyze polynya activity in the Ronne and Ross polynya regions and explore corresponding changes when FRIS and RIS cavities are opened.

S3.1 Polynya realism in the NEMO simulation without cavities

Ice production in the Ronne and Ross polynya regions in the present NEMO v4.2 eORCA1 configuration is found to overall align well with observed coastal patterns. ‘Ice production’ is diagnosed as the annual integral of sea ice generated over a domain spanning 73-80 °S and 30-60 °W for the Ronne Polynya region, and 160 °E to 155 °W south of 74 ºS for the Ross Polynya region. When FRIS melt is parameterized (“Closed” run), the Ronne Polynya region produces 24 x 10^9 m^3 of ice per year, compared to 58 ± 21 x 10^9 m^3 reported from the satellite-based estimates of Nakata et al. (2021). The Ross Polynya region produces 368 x 10^9 m^3 of ice per year in the “Closed” simulation, compared to 387 ± 41 x 10^9 m^3 reported in Nakata et al. (2021). It is important to note here that model output and satellite-based estimates are not directly comparable due to differing definitions for the region of interest between the two sources. If we look at the patterns of sea ice production (Fig. S2), we see the largest values of around 5 m yr^{-1} at the expected locations along the coasts of Antarctica (Nakata et al., 2021). Terra Nova Bay Polynya does not correspond exactly to the observed position, likely due to the absence of simulated landfast sea ice.

S3.2 Impact of explicit sub-ice shelf circulation on polynya activity

The changes in polynya activity in response to opening FRIS and RIS are minor. We find no change in the location of polynyas. Ice production does, however, slightly increase from 24 to 29 x 10^9 m^3 in the Ronne Polynya region and slightly decrease from 368 to 357 x 10^9 m^3 in the Ross Polynya region. Ice production slightly decreases to the west of the ice shelf fronts and increases eastward in both analyzed regions when cavities are opened, with changes smaller than 0.5 m yr^{-1}. Changes in ice production are consistent with simulated temperature shifts, with warming to the west and cooling to the east of FRIS and RIS (see Figs. 2 and 3) in the "Open" cavity simulation. Due to the very minor changes in volume of ice production and the absence of a location shift in polynyas, the volume of HSSW produced in each simulation is comparable. The majority of the salinity alterations observed in Figures 2i and 3i are thus likely driven by a change in circulation patterns and conversion of HSSW to ISW when the paths under the ice shelves are opened, and not by an alteration in volume of HSSW produced from polynya activity.

S3.3 Summary

Sea ice production is reasonable for the two large polynya regions we resolve (Ronne & Ross). Changes in polynya activity due to the opening of the sub-ice shelf cavities can be explained as a response to adjustments in temperature patterns. In conclusion, these effects are minor, do not change the overall locations of the polynyas, and the feedback of sea ice changes on water properties is considered weak.

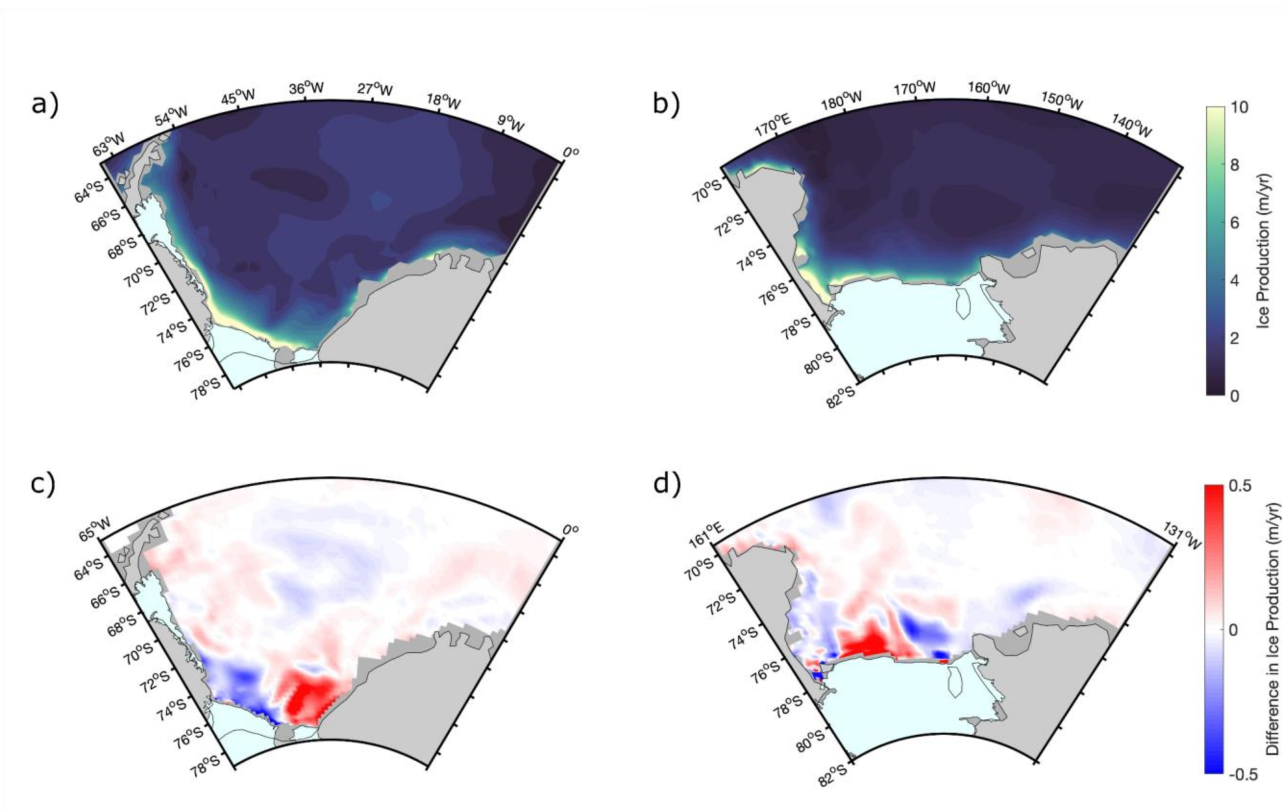

Figure S2: The annual mean sea ice production in NEMO "Closed" configuration for (a) the Weddell Sea and (b) the Ross Sea. The difference in ice production between the "Open" and "Closed" cavity runs (Open-Closed) are shown in plots (c) and (d) for Weddell and Ross seas respectively.

Data availability:

CATS2008 is available for download through the U.S. Antarctic Program Data Center: Data DOI: 10.15784/601235

References:

Howard, S., Padman, L. and Erofeeva, S.: Cats2008: Circum-antarctic tidal simulation version 2008, United States Antarctic Program Data Center 2019.

Jourdain, N. C., Molines, J., Le Sommer, J., Mathiot, P., Chanut, J., de Lavergne, C. and Madec, G.: Simulating or prescribing the influence of tides on the Amundsen Sea ice shelves, Ocean Modelling 2019.

Nakata, K., Ohshima, K. I. and Nihashi, S.: Mapping of active frazil for Antarctic coastal polynyas, with an estimation of sea-ice production, Geophys.Res.Lett. 6, 2021.

Supplementary Figures

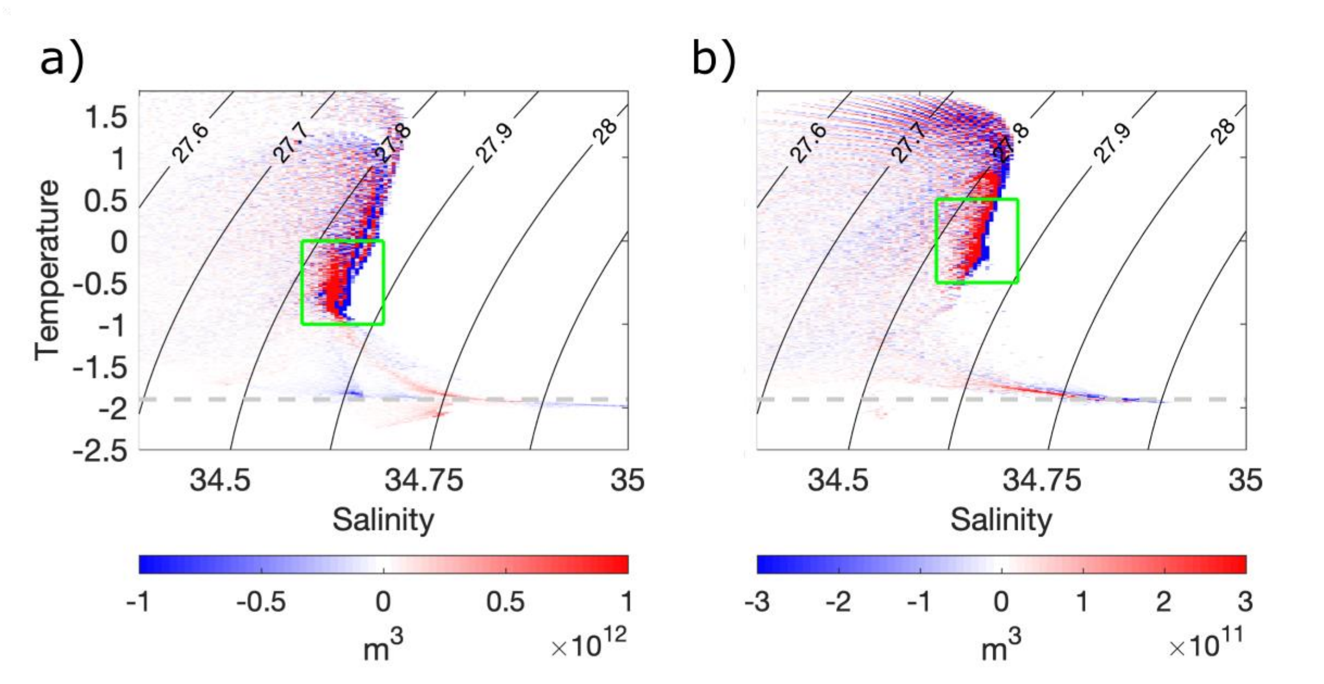

Figure S3: Difference ("Open" - "Closed") in volumetric temperature versus salinity distributions for (a) the Weddell Sea (80 - 60 °S ; 65 °W - 20 °E) and (b) the Ross Sea (85 - 68 °S; 130 °W - 160 °E) for model output excluding data underneath the ice shelves. The scatter dots are placed in T-S space according to their position in the "Closed" cavity simulation and the coloring shows the "Open"-"Closed" volumetric difference. The green boxes delimit the properties corresponding to AABW.

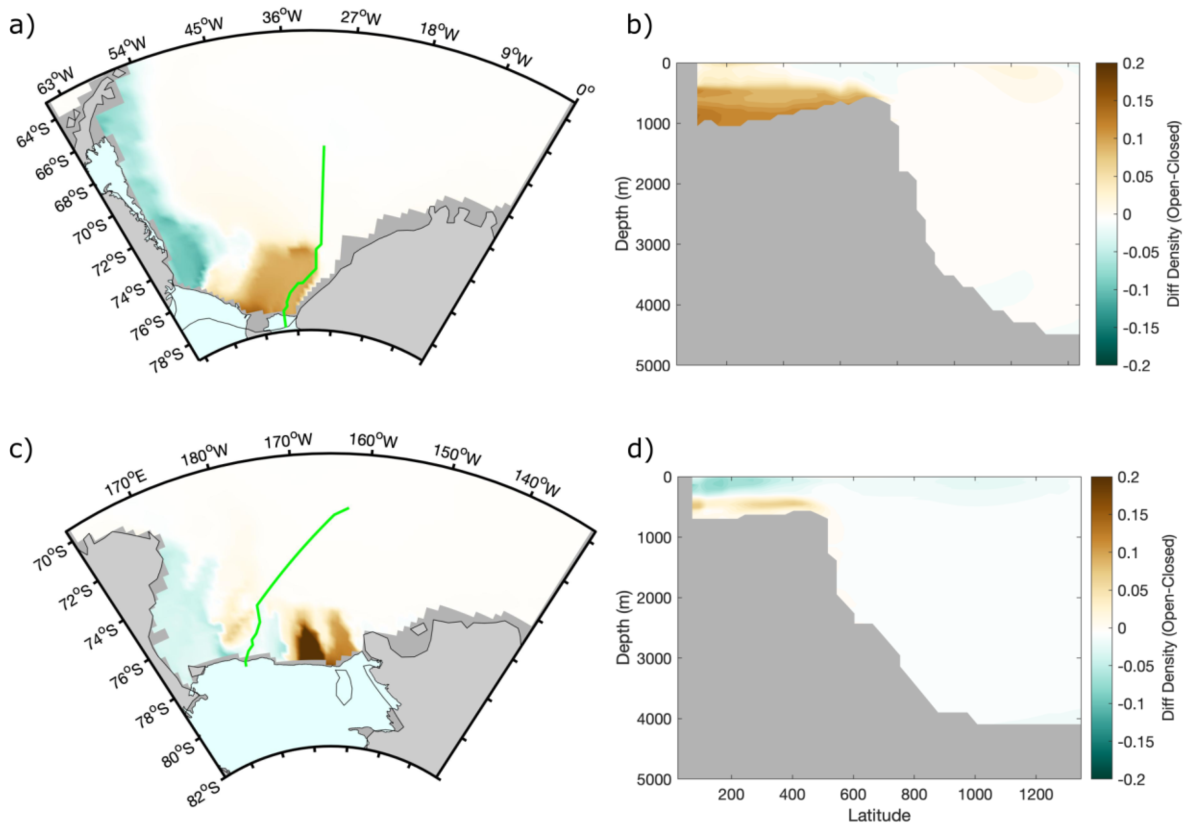

Figure S4: Density difference (kg m^{-3}) plots for the Weddell (a-b) and Ross (c-d) Seas with bottom values in subplots (a) and (c) and the cross sections of the Filchner and Challenger troughs illustrated by green lines shown in subplots (b) and (d).